A stress-triaxiality-dependent damage model and fracture criterion for aluminum alloys

M. Brünig, S. Gerke, D. Albrecht
TU Dortmund University, Dortmund, Germany;
E-mail: michael.bruenig@tu-dortmund.de

Abstract

The paper deals with the effect of stress triaxiality on the onset and evolution of damage and fracture in aluminum alloys. Comparison of results of three-dimensional finite element analyses with data obtained from smooth and pre-notched tension and shear specimens leads to a damage criterion formulated in stress space. In addition, a fracture criterion based on critical damage parameters is proposed. Different branches of these functions are taken into account corresponding to different damage and failure modes depending on stress triaxiality and Lode parameter.

1 Introduction

The accurate and realistic modeling of inelastic behavior of ductile metals is essential for the solution of numerous boundary-value problems occurring in various engineering disciplines. Great efforts have been made in the attempt to develop unified models for predicting the occurrence of damage and failure in materials and structures under general loading conditions. Within the general framework of continuum thermodynamics of irreversible processes several continuum damage models have been proposed which are either phenomenologically based or micromechanically motivated. Accurate and efficient constitutive models of damaged ductile materials are needed as the basis for an accurate theory of ductile fracture. Critical values of proposed continuum damage variables may be viewed as major parameters characterizing the onset of failure.

Besides the stress intensity, the stress triaxiality has been shown to be the most important factor that controls initiation of ductile damage. Damage conditions and damage evolution laws, however, are often validated with experimental data obtained performing uniaxial tension tests. The transferability of the identified parameters to multiaxial stress states with different stress triaxialities is not always controlled and, thus, seems to be questionable. Attempts to take into account the effect of stress triaxiality in their continuum approaches have been presented by Borvik et al. [1], Bonora et al. [2], Bai and Wierzbicki [3], and Brünig et al. [4] based on tension tests with notched specimens. Bao and Wierzbicki [5] proposed fracture strain criteria based on three different branches with shear modes for negative stress triaxialities, void-growth-dominated modes for large positive triaxialities and mixed modes for lower positive stress triaxialities. In the hydrostatic pressure regime, Bao and Wierzbicki [6] proposed a cut-off value of stress triaxiality below which damage and fracture do not occur.

2 Continuum damage and failure model

A macroscopic continuum model is used to predict the irreversible material behavior while ignoring details of the microscopic mechanics of individual voids and their interaction. Brünig [7] proposed a phenomenological framework to describe the inelastic deformations including anisotropic damage by microdefects. The approach is based on the introduction of damaged as well as corresponding fictitious undamaged configurations.

The effective undamaged configurations are considered to formulate the constitutive equations describing the effective elastic-plastic deformation behavior of the undamaged matrix material. Assuming isotropic hyperelasticity the effective stress tensor is expressed in the form

$$\bar{\mathbf{T}} = 2G\mathbf{A}^{el} + \left(K - \frac{2}{3}G\right) tr\mathbf{A}^{el}\,\mathbf{1} \tag{1}$$

where G and K represent the shear and bulk modulus of the matrix material and $\mathbf{A}^{el}$ is the elastic part of the logarithmic strain tensor.

In addition, stress-triaxiality-dependent plastic yielding of the matrix material is adequately described by the Drucker-Prager-type yield condition

$$f^{pl} = \sqrt{\bar{J}_2} - c\left(1 - \frac{a}{c}\,\bar{I}_1\right) = 0 \tag{2}$$

where $\bar{I}_1$ and $\bar{J}_2$ are invariants of the effective stress tensor $\bar{\mathbf{T}}$, c denotes the strength coefficient and a represents the hydrostatic stress coefficient where a/c is a constant material parameter. In elastic-plastically deformed and damaged metals, irreversible volumetric strains are mainly caused by damage and, in comparison, volumetric plastic strains are negligible. Thus, the isochoric effective plastic strain rate

$$\dot{\mathbf{H}}^{pl} = \dot{\gamma}\frac{1}{\sqrt{2\bar{J}_2}}\,dev\bar{\mathbf{T}} \tag{3}$$

describes the evolution of plastic deformations where $\dot{\gamma}$ is the equivalent plastic strain measure.

Furthermore, the anisotropically damaged configurations are used to formulate damaged elastic and damage constitutive equations characterizing the deformation behavior of the damaged aggregate. Experiments have shown that the existence of microdefects results in a decrease of the stress level in the aggregate and in a decrease of the elastic material properties when compared to the response of the virgin undamaged material. Thus, the stress tensor of the damaged ductile solid is given by

$$\begin{aligned}\mathbf{T} = {} & 2\left(G + \eta_2\, tr\mathbf{A}^{da}\right)\mathbf{A}^{el} + \left[\left(K - \frac{2}{3}G + 2\eta_1\, tr\mathbf{A}^{da}\right) tr\mathbf{A}^{el} + \eta_3\,\mathbf{A}^{da}\cdot\mathbf{A}^{el}\right]\mathbf{1} \\ & + \eta_3\, tr\mathbf{A}^{el}\mathbf{A}^{da} + \eta_4\left(\mathbf{A}^{el}\mathbf{A}^{da} + \mathbf{A}^{da}\mathbf{A}^{el}\right)\end{aligned} \tag{4}$$

where $\eta_1 \ldots \eta_4$ are material parameters taking into account the deterioration of the elastic properties due to the occurrence of damage [7] and $\mathbf{A}^{da}$ denotes the damage part of the strain tensor.

In addition, constitutive equations for damage evolution are required and the determination of onset and continuation of damage is based on the concept of

damage surface. In pure shear and compression tests which are in the range of zero or low negative stress triaxialities shear mechanisms dominate. In this regime the onset of damage is assumed to be governed by the damage criterion

$$f^{da} = \sqrt{J_2} - \sigma = 0 \qquad \text{for} \qquad \frac{-1}{3} \le \eta \le 0 \tag{5}$$

where σ denotes the damage threshold stress representing the material toughness to microdefect propagation and the stress triaxiality $\eta = \sigma_m / \sigma_{eq} = I_1 / \left(3\sqrt{3J_2} \right)$ is defined as the ratio of the mean normal stress and the von Mises equivalent stress. This regime of low stress triaxialities is limited by the cut-off value of negative stress triaxialities $\eta = -1/3$ and the value of transition to the mixed-mode regime is $\eta = 0$.

In the range of high positive stress triaxialities damage is mainly caused by void growth. In this regime the onset of damage is suggested to be governed by the damage criterion

$$f^{da} = \frac{1}{3} I_1 - \sigma = 0 \qquad \text{for} \qquad \eta \ge \frac{1}{\sqrt{3}} \tag{6}$$

and the value of transition to the mixed-mode regime is $\eta = 1/\sqrt{3}$.

At stress triaxialities between the above two regimes damage may develop as a combination of shear and void growth modes. In this regime, the onset of damage is assumed to be governed by the damage criterion

$$f^{da} = \frac{1}{3} I_1 + \beta\sqrt{J_2} - \sigma = 0 \qquad \text{for} \qquad 0 < \eta < \frac{1}{\sqrt{3}}. \tag{7}$$

The damage mode parameter

$$\beta = 1 - \sqrt{3}\,\eta + d\omega \tag{8}$$

describes the dependence of damage initiation on stress triaxiality and Lode parameter

$$\omega = \frac{2\tilde{T}_2 - \tilde{T}_1 - \tilde{T}_3}{\tilde{T}_1 - \tilde{T}_3} \qquad \text{with} \qquad \tilde{T}_1 \ge \tilde{T}_2 \ge \tilde{T}_3 \tag{9}$$

expressed in terms of the principal stress components $\tilde{T}_1, \tilde{T}_2$ and $\tilde{T}_3$.

Alternatively, Brünig et al. [4] proposed the damage mode parameter

$$\beta = 1 - \left(d\eta \right)^m \tag{10}$$

only depending on stress triaxiality. In Eqs. (8) and (10) *d* and *m* represent additional material parameters.

The damage evolution law models the increase in macroscopic strains caused by the simultaneous growth of voids, their coalescence as well as the evolution of micro-cracks and micro-shearbands leading to anisotropic damage behavior. This will be adequately described by the damage rule

$$\dot{\mathbf{H}}^{da} = \dot{\mu} \left(\frac{1}{3} \frac{1-\beta}{1-f} \mathbf{1} + \beta \frac{1}{2\sqrt{J_2}}\, dev\tilde{\mathbf{T}} \right) \tag{11}$$

which takes into account isotropic and anisotropic parts, $\dot{\mu}$ is the rate of the equivalent damage strain measure and $\tilde{\mathbf{T}}$ denotes the stress tensor work-conjugate to the damage strain rate $\dot{\mathbf{H}}^{da}$ [7].

It should be noted that in the high stress triaxiality regime $\eta \geq 1/\sqrt{3}$ first damage is caused by nearly isotropic growth of voids and anisotropic effects occur later due to the coalescence of voids. This transition from the isotropic to the mixed damage mode with simultaneous further growth and coalescence of voids is often predicted by a critical void volume fraction (see [7] for further details) depending on initial porosity and, in the considered generalized case, on stress triaxiality. This will lead to an increase in damage mode parameter β with increasing damage.

The transition from micro-defects to macro-cracks is assumed to be adequately described by the failure criterion

$$f^{fail} = \frac{1}{3} I_1^{da} + \beta \sqrt{J_2^{da}} - \mu_{cr} = 0 \tag{12}$$

formulated in terms of the first and second deviatoric invariants I_1^{da} and J_2^{da} of the damage strain tensor $\mathbf{A}^{da}$. In Eq. (12), μ_{cr} denotes the critical equivalent damage strain measure. The onset and evolution of macro-cracks is numerically modeled by an element erosion technique.

3 Numerical simulations

Numerical simulations of various tension and shear tests are performed. Driemeier et al. [8] discussed experiments on pre-notched tension and pre-notched shear specimens taken from a 6.35mm thick plate of aluminum alloy. These tests provide a wide range of stress triaxialities. In addition, unnotched specimens were tested to obtain the basic elastic-plastic material parameters.

Figure 1 shows the geometries and finite element meshes of the pre-notched shear specimen (a) with a circular channel of 1.0mm depth (detail b) and of the pre-notched tension specimen with 20mm notch radius (c). Using symmetry conditions, only half of the shear specimen and an eighth part of the tension bar are numerically analyzed. Eight-node volumetric elements are used to three-dimensionally discretize the 6.35mm thick specimens. Remarkable refinements in the thin regions have been taken into account where evolution of plastic zones and first occurrence of damage and failure are expected.

Tension tests with smooth specimens (UN-T6.35) are considered for identification of elastic-plastic material parameters. As long as a homogeneous uniaxial stress state exists between the clip gauges, equivalent stress-equivalent strain relations can easily be predicted from load-displacement curves of these experiments. This leads to Young's modulus E = 75000 MPa and Poisson's ratio is taken to be $\nu = 0.3$. Work-hardening behavior during plastic yielding is modeled by a power law function for the equivalent effective stress

$$c = c_0 \left(\frac{H\gamma}{n c_0} + 1 \right)^n \tag{13}$$

with the initial yield strength c_0 = 250MPa, the hardening modulus H = 3125MPa and the hardening exponent n = 0.135. Of course, necking occurs during the elongation of the originally smooth tension specimen which might cause necking induced variations in the initially quasi-homogeneous stress and plastic strain states. Thus, 3D-finite element simulations of the smooth tension tests have been performed which here confirmed the chosen material parameters.

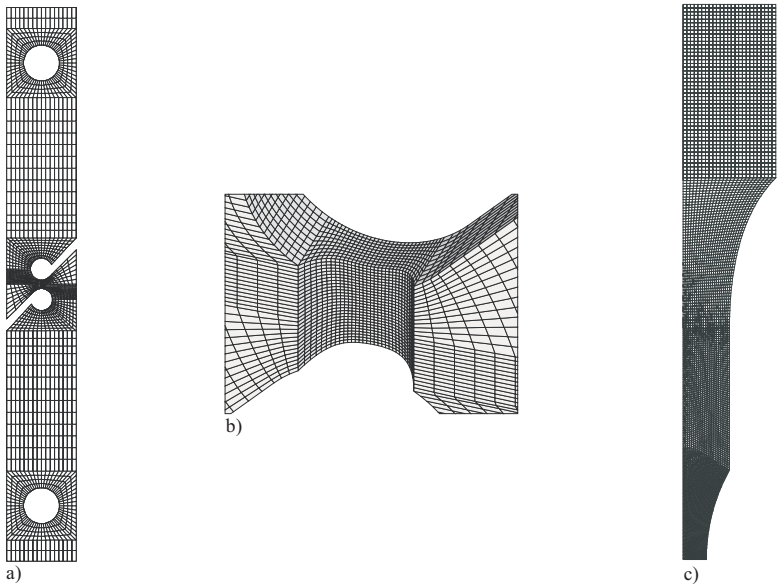

Figure 1: Finite element meshes: a) Shear specimen, b) Detail of pre-notched part of the shear specimen, c) Tension specimen.

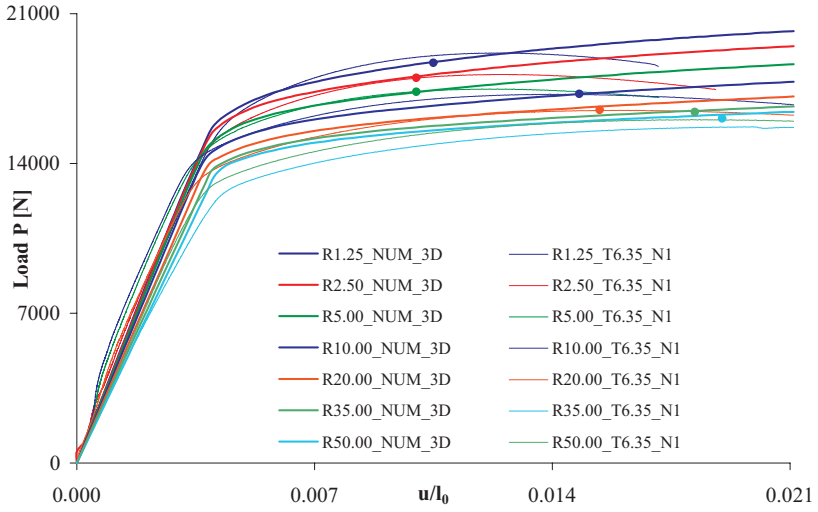

Figure 2: Load-engineering strain curves of tension tests: Experimental (T6.35) and numerical (NUM) results as well as onset of damage (dot)

Tension tests with pre-notched specimens with different notch radii from 1.25mm to 50mm (see Fig. 2) are investigated to study the effect of stress triaxiality and Lode parameter on damage behavior. Usually, various unloading paths are driven during the tension tests to be able to detect the damage by decreasing Young's modulus. This procedure, however, has been shown to be very difficult for the tested aluminum alloy and, especially, for the pre-notched specimens because the onset of damage is close to final fracture. Therefore, Brünig et al. [4] proposed an alternative method to detect the onset of damage. They performed elastic-plastic finite element calculations and the observed discrepancy between experimentally obtained and numerically predicted load-displacement curve characterizes the onset of damage.

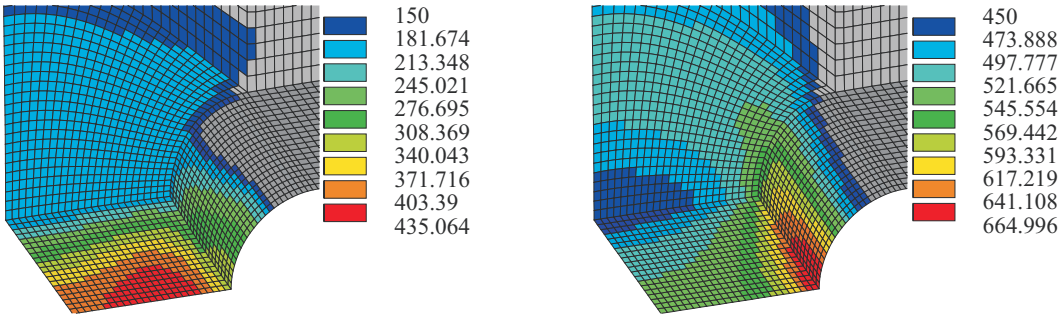

Figure 3: Numerical results: Hydrostatic stress and von Mises equivalent stress

Based on the elastic-plastic material parameters identified above the correlation of experimental and numerical results is very good in terms of the load-displacement curves shown in Fig. 2. The onset of damage can be identified (dots in Fig. 2) and, thus, it is reasonable to study at this stage of deformation various stress quantities obtained from the numerical analyses. Figure 3 shows the distribution of hydrostatic stress $1/3\ I_1$ and von Mises equivalent stress $\sqrt{3J_2}$ at the onset of damage in the notched center of the tension specimen with 1.25mm notch radius. In this high-stress-triaxiality case, onset of damage is predicted in the point of maximum hydrostatic stress in the inner region of the cross section (lower and left bounds are symmetry axes). It should be noted that these results clearly show that 3D finite element analyses are necessary because both stress measures remarkably vary over the cross section and maximum values are concentrated in small points.
Moreover, shear tests are analyzed to get information of the effect of state of stress on damage in the region of very low stress triaxialities. Load-engineering strain curves in Fig. 4 show good agreement between experimental and numerical results. The onset of damage is predicted and distributions of stress measures are shown in Fig. 5 for the shear specimen with 1.0mm notch depth. Maxima of hydrostatic stresses are concentrated on the surfaces of the holes whereas the center is nearly free of hydrostatic stress leading to pure shear-mode behavior. Maxima of von Mises equivalent stress are also concentrated in the center. Thus, onset of damage is predicted to occur in this point.

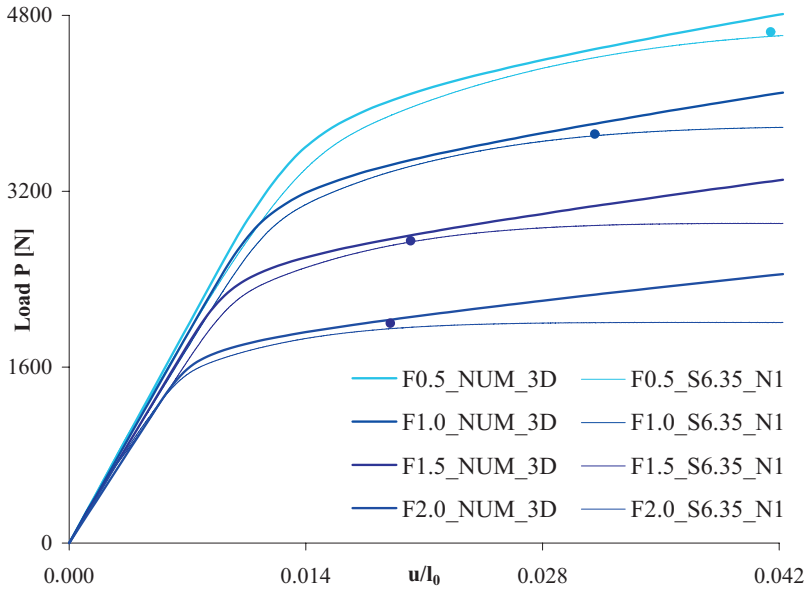

Figure 4: Load-engineering strain curves of shear tests: Experimental (S6.35) and numerical (NUM) results as well as onset of damage (dot).

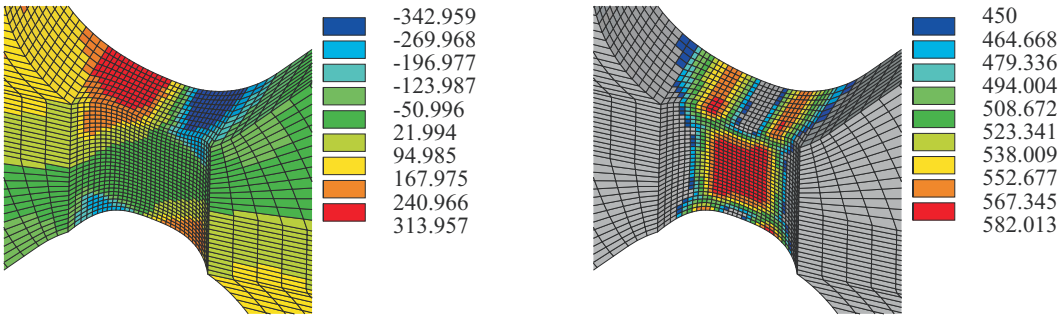

Figure 5: Numerical results: Hydrostatic stress and von Mises equivalent stress

Various stress data introduced above are listed in Table 1 for smooth and pre-notched specimens. These data are used to identify the parameters of the damage evolution functions (Eqs. (8) and (10), respectively) shown in Fig. 6. The parameters are d = -0.015 in Eq. (8), and d = 1.732 and m = 1.18 in Eq. (10).
The stress data listed in Table 1 show remarkable influence of specimen's geometry on the first stress invariant characterizing the hydrostatic stress whereas the second deviatoric stress invariant is nearly unaffected. This leads to remarkably wide range of stress triaxiality parameters covered by these tests. Furthermore, in the thick notched tension specimens with nearly quadratic cross section necking in thickness direction is observed during the tension tests leading to three-dimensional stress states, see list of principal stresses in Tab. 1. In addition, thickness effects are also observed in the shear tests with pre-notched specimens. Their different geometries lead to wide range of Lode parameters covered by these tests. Therefore, the numerical simulations discussed above will

be helpful in detecting stress-triaxiality and Lode-parameter dependence of material behavior.

	I_1	$\sqrt{J_2}$	$\sqrt[3]{J_3}$	η	$\tilde{T}_1$	$\tilde{T}_2$	$\tilde{T}_3$	ω
R1.25_T6.35	1304	316	223	0.7927	796	299	209	-0.6951
R2.50_T6.35	1159	309	202	0.7213	732	291	136	-0.4584
R5.00_T6.35	1047	314	225	0.6416	710	200	137	-0.7760
R10.00_T6.35	902	343	249	0.5067	696	112	94	-0.9421
R20.00_T6.35	755	332	242	0.4374	635	62	58	-0.9845
R35.00_T6.35	671	332	241	0.3890	607	33	32	-0.9959
R50.00_T6.35	630	325	237	0.4708	586	22	22	-0.9986
UNN_T6.35	518	299	217	0.3333	518	0	0	-1.0000
UNN_S6.35	1041	365	179	0.5483	732	304	5	-0.1788
F0.50_S6.35	765	342	241	0.4304	646	101	9	-0.6831
F1.00_S6.35	19	336	85	0.0108	345	1	-327	-0.0241
F1.50_S6.35	7	314	62	0.0046	318	0	-311	-0.0116
F2.00_S6.35	7	321	62	0.0041	325	0	-318	-0.0108

Table 1: Stress data at onset of damage

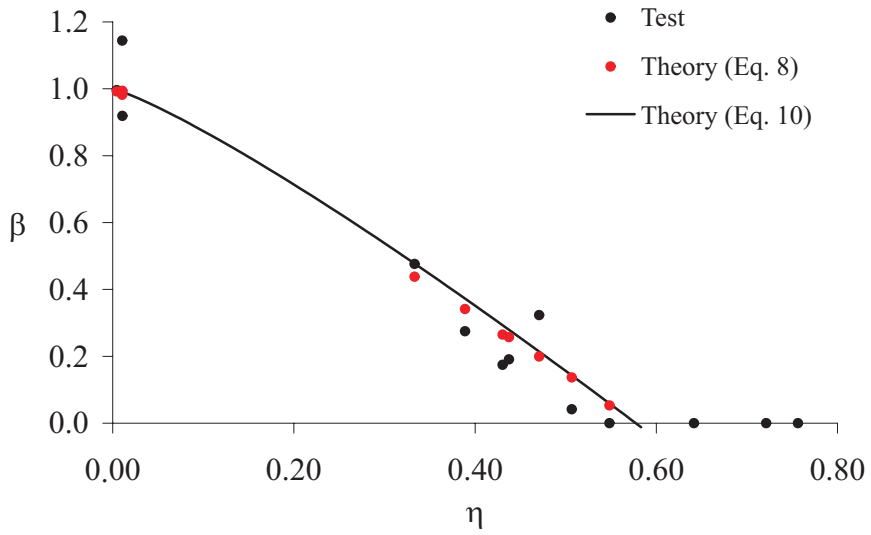

Figure 6: Damage mode parameter vs. stress triaxiality

4 Conclusions

The main focus of the present paper was to discuss a general methodology for quantitative determination of damage and failure criteria for any ductile metal. A series of numerical simulations of experiments with smooth and pre-notched tension and shear specimens have been carried out covering a wide range of stress triaxialities. Different branches of the criteria have been proposed corresponding to different failure modes depending on stress triaxiality and Lode parameter.

References

[1] T. Borvik, O.S. Hopperstad, T. Berstad, On the influence of stress triaxiality and strain rate on the behavior of a structural steel. Part II. Numerical study, Eur. J. Mech. A/Solids 22 (2003), 15-32

[2] N. Bonora, D. Gentile, A. Pirondi, G. Newaz, Ductile damage evolution under triaxial state of stress: theory and experiment, Int. J. Plast. 21 (2005), 981-1007

[3] Y. Bai, T. Wierzbicki, A new model of metal plasticity and fracture with pressure and Lode dependence, Int. J. Plast. 24 (2008), 1071-1096

[4] M. Brünig, O. Chyra, D. Albrecht, L. Driemeier, M. Alves, A ductile damage criterion at various stress triaxialities, Int. J. Plast. 24 (2008), 1731-1755

[5] Y. Bao, T. Wierzbicki, On fracture locus in the equivalent strain and stress triaxiality space, Int. J. Mech. Sci. 46 (2004), 81-98

[6] Y. Bao, T. Wierzbicki, On the cut-off value of negative triaxiality for fracture, Eng. Frac. Mech. 72 (2005), 1049-1069

[7] M. Brünig, An anisotropic ductile damage model based on irreversible thermodynamics, Int. J. Plast. 19 (2003), 1679-1713

[8] L. Driemeier, M. Brünig, G. Micheli, M. Alves, Experiments on stress-triaxiality dependence of material behavior of aluminum alloys (submitted).